DOI: 10.58895/ksp/1000128686-5 erschienen in:
OCM 2021 - 5th International Conference on Optical Characterization of Materials, March 17th – 18th, 2021, Karlsruhe, Germany : Conference Proceedings
DOI: 10.58895/ksp/1000128686 | https://www.ksp.kit.edu/site/books/m/10.58895/ksp/1000128686/

Detection of pyrrolizidine alkaloid containing herbs using hyperspectral imaging in the short-wave infrared

Julius Krause[1], Nanina Tron[2], Georg Maier[1], Andrea Krähmer[2], Robin Gruna[1], Thomas Längle[1], and Jürgen Beyerer[1,3]

[1] Fraunhofer IOSB, Karlsruhe, Institute of Optronics, System Technologies and Image Exploitation, Visual Inspection Systems, Fraunhoferstr. 1, 76131 Karlsruhe, Germany
[2] Julius Kühn-Institut (JKI), Federal Research Centre of Cultivated Plants, Institute for Ecological Chemistry, Plant Analysis and Stored Product Protection, Königin-Luise-Str. 19, 14195 Berlin, Germany
[3] Karlsruhe Institute of Technology (KIT), Vision and Fusion Laboratory (IES), Haid-und-Neu-Str. 7, 76131 Karlsruhe, Germany

Abstract Plants containing pyrrolizidine alkaloids (PA) are unwanted contaminants in consumer products such as herbal tea due to their toxicity to humans. The detection of these plants or their components using hyperspectral imaging was investigated, with focus on application in sensor-based sorting. For this, 431 hyperspectral images of leafs from three common herbs (peppermint, lemon balm, stinging nettle) and the poisonous common groundsel were acquired. By using a convolutional neural network, a mean F_1 score of 0.89 was obtained for the classification of all four plant products based on the individual spectra. To validate the neural network, significant wavelengths were determined and visualized in an attribution map.

Keywords Hyperspectral Imaging, convolutional neural network, Pyrrolizidine alkaloids, sensor-based sorting

1 Introduction

Pyrrolizidine alkaloids (PA) are secondary plant substances that are toxic to the genome and the liver. They can pose a health hazard, as they are often found as a contaminant in food or medicinal plant products. Just a few plants per hectare e.i. of *Senecio* are sufficient to contaminate the product non marketable. Hence, regular field monitoring and removal of appropriate weeds is necessary. This is a considerable personnel effort that can hardly be afforded economically by the growers. Additionally, for correct identification of toxic herbs and to prevent contamination of the products, the growers need well trained personal. Therefore, methods to identify and remove toxic contaminants after harvest are highly demanded.

Sensor-based sorting is a machine vision application that has found industrial application in various fields. An accept-or-reject task is executed by deflecting single particles from a material stream. The main fields of application of sensor-based sorting are recycling, e.g., removing materials from glass shard streams harmful to the melting process such as stones and ceramic glass [1]. Another field of application is the processing of industrial minerals, mainly to remove unwanted gangue from ore, e.g., copper-gold ore [2]. For ensuring product safety for foodstuff and agricultural products, these methods are used for the detection and removal of fungus-infected wheat kernels [3]. Hence, sensor-based sorting of crops also represents an opportunity to safe the harvest potentially contaminated with PA.

In this paper, three of the economically most important herb cultures in Germany (peppermint, lemon balm, stinging nettle) and the most common contaminant of these cultures (common groundsel) were characterized by near infrared spectroscopy. Optical spectroscopy in near and short-wave infrared is particularly suitable for the detection and differentiation of organic products. Using hyperspectral camera systems, material streams can be monitored and foreign substances can be separated after detection by implementing the techniques in a sensor-based sorting system. Targeting this application, hyperspectral data was acquired for the mentioned herbs and their frequent contamination in an experimental sensor-based sorting system.

2 Material and methods

This section describes the experimental sensor-based sorting system that was used to acquire the data. In addition, insights into the resulting data set are given. Finally, the novel data analysis method for the task at hand is described.

2.1 Experimental sensor-based sorting platform with hyperspectral camera system

In the course of this study, data for different plants are acquired using an experimental sorting platform that is equipped with an hyperspectral camera system, see Fig. 2.1. A thorough description of the experimental platform is provided in [4]. The spectral sensitivity of the InGaAs sensor of the line-scanning hyperspectral camera lies in the range of approximately 1200 to 2200 nm that is sampled into 256 spectral bands and provides 320 pixels locally at a maximal temporal resolution of approximately 300 hz. The implemented illumination consists of two arrays of halogen spotlights, which are locally targeted at the scan-line of the camera. Transportation of the material is realized by means of a conveyor belt that runs at 1.1 ms^{-1}. The material is observed directly after being discharged from the belt, i. e., during a free flight phase. An array of pneumatic nozzles is located behind this scan-line and serves the purpose of material separation. It consists of 16 nozzles that can be triggered individually, each of which covering a width of 10 mm.

2.2 Dataset

The plant material for the measurements was cultivated in beds at the JKI Berlin. The medicinal cultures were harvested twice, each time at the beginning of flowering, as the concentration of essential oils is highest then, using a cutting height of approx. 15 cm. For lemon balm (*Melissa officinalis*) and peppermint (*Mentha x piperita* 'Multimentha') 24 each and for stinging nettle (*Urtica dioica*) 12 and for groundsel (Senecio vulgaris) 10 single plants were harvested.

For training, the data set was split by random sample selection. A ratio of 75% was assigned as training and of 25% as validation data.

Figure 2.1: Photo of the experimental sensor-based sorting platform, equipped with the hyperspectral camera system.

Table 5.1: Description of the resulting dataset.

name	trivialis	samples	spectra
Senecio vulgaris	groundsel	84	44683
Urtica dioica	stinging nettle	98	34447
Melissa officinalis	lemon balm	141	17747
Mentha piperita	peppermint	108	15970

The entire data set can be described with a matrix $\boldsymbol{X} := \{\vec{x}_i\}_{i=1..N}$ of N spectra and a matrix $\boldsymbol{Y} := \{\vec{y}_i\}_{i=1..N}$ of N labels. Each spectrum $\vec{x}_i \in \mathbb{R}^Q$ contains the reflectance of $Q = 256$ spectral bands. The labels $\vec{y}_i \in \mathbb{R}^C$ are coded as one-hot vectors with $C = 4$ classes, which correspond to the plant types. An exemplary visualization of the data is shown in Fig. 2.2.

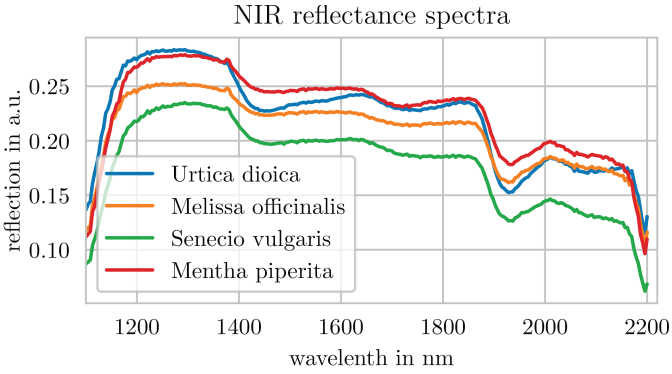

Figure 2.2: Shown are the mean spectra of all four plant species. Through the intensity differences at certain wavelengths, a classification can be done.

2.3 Data analysis using the convolutional neural network *AnniNet*

A new neural network architecture, *AnniNet*, has been developed at Fraunhofer IOSB. This architecture is particularly suitable for the analysis of near-infrared spectra. *AnniNet* consists of three components, namely an encoder network for feature extraction, a decoder network to improve feature extraction and a classification network that estimates the class membership of a spectrum. All three networks are trained in parallel through multi-task learning. The feature extraction structure does not require any type of spectral data pre-processing. The individual parts of *AnniNet* and multi-task learning are presented in the following.

Encoder network

The encoder layer is used for feature extraction. For this purpose, a layer with different one-dimensional convolution kernels is trained and applied to the spectrum. This layer can be compared with wavelet-based methods that are already successfully used in chemometrics [5]. It has been shown that wavelets are successful in reducing noise [6] and suppressing background effects [7]. This enabled improved results [8], even the transfer of chemometric models was improved [9]. The features determined by means of the convolutional layer are sent to

a pooling layer. This layer has a very practical effect besides reducing the parameters for the following layers. The feature extraction becomes more robust against shifts in the wavelength. This is especially a disturbing effect known as smiley keystone distortion in hyperspectral cameras.

Decoder network

End-to-end learning in artificial neural networks with high dimensional inputs such as hyperspectral measurements requires a large amount of labeled training samples due to a high count of weights which are iteratively adjusted. Autoencoders are used to learn the representation of a dataset in a unsupervised manner. Adding a decoder network creates such an autoencoder within *AnniNet* and improves training results without the need for additional labels.

Classification network

To evaluate the overlapping information from the individual absorption bands, fully connected (dense) layers were used. In correspondence with the exponential behavior of absorption processes (Beer-Lambert law), the Scaled Exponential Linear Units (SELU) activation function

$$f(x) = \begin{cases} \lambda\alpha(e^x - 1), & \text{if } x < 0 \\ \lambda x, & \text{otherwise} \end{cases} \tag{2.1}$$

was chosen for the first dense layer. Finally, a fully connected layer with the softmax activation function is applied. The output of the classification network is a normalized probability density function of the estimated class memberships.

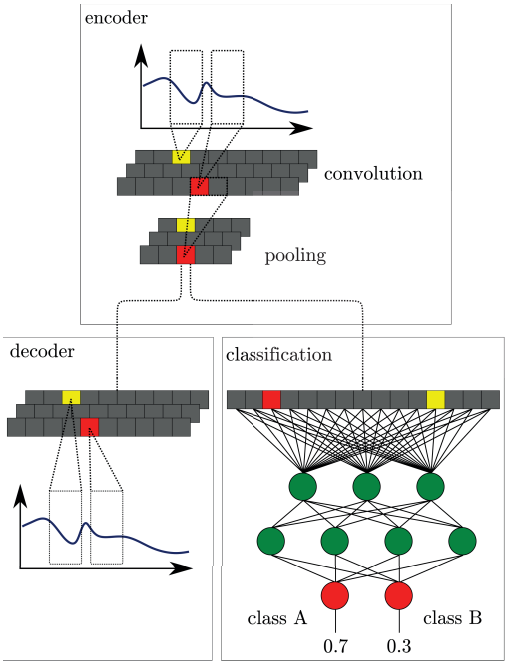

Figure 2.3: *AnniNet* consists of three components. First, an encoder network extracts spectral features using a convolutional layer. During training, a decoder network is used as an autoencoder to improve feature extraction. The classification network analyses the non-linear and overlapping spectral features.

Multi-task-learning

Using multi-task-learning, all four classes and the reconstruction of the autoencoder were trained in parallel. The categorical cross entropy

$$\mathrm{CCE} = -\frac{1}{N}\sum_{i=1}^{N}\sum_{j=1}^{C} y_{i,j}\log\hat{y}_{i,j} \tag{2.2}$$

was used as a loss function to optimize the classification results for all classes C. The reconstruction of the spectral data using the autoencoder

was optimized by minimizing the Root Mean Square Error

$$\mathrm{RMSE} = \frac{1}{N}\sum_{i=1}^{N}\sqrt{\frac{\sum_{j=1}^{Q}(\hat{x}_{i,j} - x_{i,j})^2}{n}} \tag{2.3}$$

for the autoencoder, which improves the feature extraction.

3 Results and discussion

The classification was carried out using *AnniNet* without any spectral pre-processing. To validate the results in the following, only spectra from samples that were not included in the training were used. To check the plausibility of the classification results, a sensitivity analysis was performed and compared with the spectral data.

3.1 Classification results

The results of the classification are shown in the confusion matrix in Fig. 3.1. For all classes, the classification achieves a rather high accuracy. The application of a majority vote for the respective samples has led to a completely correct mapping in the validation data set. The quality of the classification results can be quantified by the so-called F_1 score

$$F_1 = \frac{\mathrm{tp}}{\mathrm{tp} + 0.5(\mathrm{fp} + \mathrm{tp})}, \tag{3.1}$$

which is the harmonic mean of precision and recall. The evaluation calculation is based on the false (fp) and true (tp) positive classification results. For the present four-class classification, the F_1 score was determined for the individual classes and averaged. The score determined in this way is $F_1 = 0.89$.

3.2 Spectral attribution map

Neural networks cannot be interpreted by humans due to their high number of parameters and high-dimensional transformations. However, when evaluating hyperspectral data, it is interesting to see which

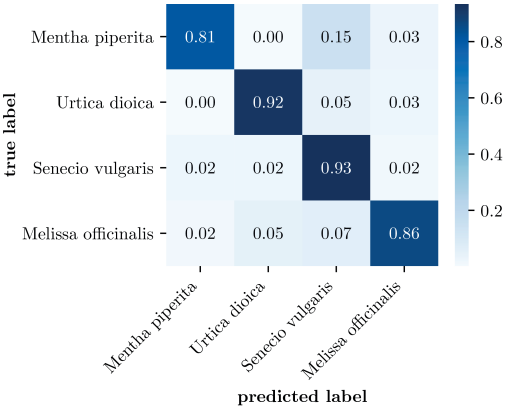

Figure 3.1: The normalised confusions matrix shows the probabilities of the estimated class memberships in the individual fields. The estimation of the class membership by single spectra is mostly correct. It is important here that by majority vote of all spectra of a sample, all test samples could be correctly classified.

absorption bands have an influence on the classification result. One possibility for investigating neural networks is the creation of a so-called attribution map. For this purpose, individual areas of the spectrum are successively masked and then the classification quality is evaluated. For the classification task at hand, such attribution maps were determined and are visualized in Fig. 4.1. As can be seen, the classification result is mainly depend on data in the range between 1400 nm and 1900 nm. This range is between the absorption's by water and can therefore be considered robust. In addition, areas are selected or weighted differently for the different class memberships, which is another indicator of robust classification.

4 Summary

Leaves from four different plants were recorded with a hyperspectral camera built in a senor-based sorting system. The data were used without spectral pre-processing to train a neural network designed for this classification task. The trained network was able to predict individual spectra of the validation data of all four classes at a high accuracy. Us-

ing a majority vote per sample, all validation samples were correctly classified. An attribution map was used to investigate which spectral ranges dominate the classification decision. The result shows different spectral ranges for the individual classes, apart from absorption by water.

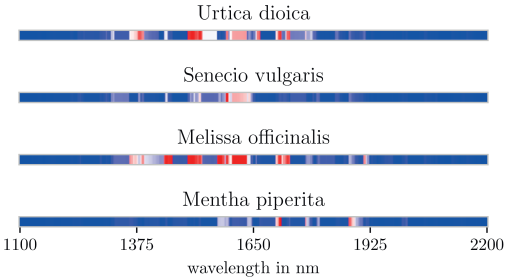

Figure 4.1: The attribution maps show the classification error caused by masking out individual spectral channels, highlighting the importance of information in the range of 1400 nm and 1900 nm.

Acknowledgement

The authors of this work were supportet by the joint project "Detektion und Entfernung von Pyrrolizidinalkaloid-haltigen Unkräutern aus Kulturpflanzen nach der Ernte – PA-NIRSort" which is funded by the German Federal Ministry of Food and Agriculture and by the Fachagentur für Nachwachsende Rohstoffe e. V. (FNR) (FKZ 220132165) on the basis of a resolution of the German Bundestag and the Fraunhofer Center for Machine Learning within the Fraunhofer Cluster of Excellence Cognitive Internet Technologies CCIT.

References

1. G. Bonifazi and S. Serranti, "Imaging spectroscopy based strategies for ceramic glass contaminants removal in glass recycling," *Waste Management*, vol. 26, no. 6, pp. 627–639, Jan. 2006. [Online]. Available: http://www.sciencedirect.com/science/article/pii/S0956053X05001649

2. T. Phiri, H. J. Glass, and P. Mwamba, "Development of a strategy and interpretation of the NIR spectra for application in automated sorting," *Minerals Engineering*, vol. 127, pp. 224–231, Oct. 2018. [Online]. Available: http://www.sciencedirect.com/science/article/pii/S0892687518303522

3. S. R. Delwiche, T. C. Pearson, and D. L. Brabec, "High-Speed Optical Sorting of Soft Wheat for Reduction of Deoxynivalenol," *Plant Disease*, vol. 89, no. 11, pp. 1214–1219, Nov. 2005. [Online]. Available: http://apsjournals.apsnet.org/doi/abs/10.1094/PD-89-1214

4. G. Maier, F. Pfaff, C. Pieper, R. Gruna, B. Noack, H. Kruggel-Emden, T. Längle, U. D. Hanebeck, S. Wirtz, V. Scherer *et al.*, "Experimental evaluation of a novel sensor-based sorting approach featuring predictive real-time multiobject tracking," *IEEE Transactions on Industrial Electronics*, vol. 68, no. 2, pp. 1548–1559, 2020.

5. C. B. Singh, R. Choudhary, D. S. Jayas, and J. Paliwal, "Wavelet analysis of signals in agriculture and food quality inspection," *Food and Bioprocess Technology*, vol. 3, no. 1, pp. 2–12, 2010.

6. C. R. Mittermayr, S. G. Nikolov, H. Hutter, and M. Grasserbauer, "Wavelet denoising of Gaussian peaks: A comparative study," *Chemometrics and Intelligent Laboratory Systems*, vol. 34, no. 2, pp. 187–202, 1996.

7. H. Tan, S. T. Sum, and S. D. Brown, "Improvement of a standard-free method for near-infrared calibration transfer," *Applied Spectroscopy*, vol. 56, no. 8, pp. 1098–1106, 8 2002.

8. X. Fu, G. Yan, B. Chen, and H. Li, "Application of wavelet transforms to improve prediction precision of near infrared spectra," *Journal of Food Engineering*, vol. 69, no. 4, pp. 461–466, 2005.

9. J. Trygg and S. Wold, "PLS regression on wavelet compressed NIR spectra," *Chemometrics and Intelligent Laboratory Systems*, vol. 42, no. 1-2, pp. 209–220, 1998.